ALCHEMY Jurnal Penelitian Kimia

Official Website: https://jurnal.uns.ac.id/alchemy

ISSN 1412-4092
EISSN 2443-4183

Optimization Depolymerization of Tilapia Fish Scale Chitosan by Oxidative Degradation with H_2O_2 using Central Composite Design (CCD)

Dhian Eka Wijaya[a*], Afra Raeviana Putri[b], Intan Lestari[a], Edwin Permana[c], Munifilia Ekasari[a], Nur Ahniyanti Rasyid[d]

[a]*Department of Chemical Analysis, Faculty of Science and Technology, Jambi University*
[b]*Department of Chemistry, Faculty of Science and Technology, Jambi University*
[c]*Department of Industrial Chemistry, Faculty of Science and Technology, Jambi University*
Jalan Jambi-Ma.Bulian. Km.15, Jambi, 36361, Indonesia
[d]*Department of Actuarial Science, Faculty of Science and Technology, Jambi University*
Jalan Poros Bulukumba - Bantaeng, Mariorennu, Gantarang, Sulawesi Selatan 92561, Indonesia

[*]*Corresponding author: dhianekawijaya@unja.ac.id*

DOI: 10.20961/alchemy.22.1.95765.95-105

Received 2 December 2024, Revised 12 September 2025, Accepted 12 December 2025, Published 31 March 2026

Keywords:

central composite design (CCD); chitosan; depolymerization; fish scales; oligochitosan.

ABSTRACT. Tilapia fish scales are among the fishery wastes that have not been optimally utilized, even though they have economic potential when processed into chitosan. Chitosan is a poly(2-amino-2-deoxy-β-D-glucose) obtained by deacetylation of chitin, with a high molecular weight ranging from 100 to 1.200 kDa, making it difficult to dissolve in water. To increase its solubility, chitosan can be depolymerized into oligochitosan with a lower molecular weight, around 5 – 10 kDa. This depolymerization process is influenced by temperature, time, and concentration factors. This study aims to determine the optimal conditions for the depolymerization of chitosan from tilapia fish scales using a central composite design (CCD). The stages of chitosan production include demineralization, deproteinization, and deacetylation, yielding a white powder with a molecular weight of 264.214 kDa and a degree of deacetylation of 74.24%. Based on CCD optimization, the optimal conditions for the depolymerization of tilapia fish scale chitosan were 3.6 M H_2O_2, 50 °C, and 2 hours, yielding a molecular weight of 3093 kDa. Fourier transform infrared (FTIR) characterization showed a peak shift from wave number 3267 cm^{-1} to 3303 cm^{-1}. Oligochitosan also showed 100% solubility in water at neutral pH.

INTRODUCTION

Indonesia's vast waters produce abundant fish, resulting in high annual fish production. Until 2023, data from the Directorate General of Fisheries and Aquaculture show that fishery production reached 18.5 million tons, split between capture and aquaculture fisheries, with tilapia (*Oreochromis niloticus*) as its flagship product. Tilapia is a tough, fast-growing freshwater fish widely cultivated in Indonesia for its resistance to disease and adaptability to various environments, including lakes, rivers, and fish ponds (Saleh *et al.*, 2021). However, the high production of tilapia is also associated with significant waste.

Tilapia processing produces liquid and solid waste, with fish scales being the main component of the solid waste. Suboptimal waste management can cause various problems, including water pollution, bad odors, and negative impacts on the environment, health, and social life of the community (Susanti and Purwanti, 2020). Recognizing the challenges of managing tilapia scale waste, recent studies have focused on its use as a value-added product. One way this can be done is by producing chitosan derived from chitin in tilapia scales. Chitosan, a product of chitin deacetylation, has a wide range of applications. However, its use is often hampered by its high molecular weight (100 – 1,200 kDa), which limits solubility at pH below 6.3 or at neutral pH (Mahardika *et al.*, 2020).

This condition underscores the need to modify chitosan through depolymerization to expand its function by producing oligochitosan, which are chitosan with low molecular weight. The product exhibits increased solubility and bioactivity, including better antibacterial properties. In general, oligochitosan can be made from chitosan with

Cite this as: Wijaya, D. E., Putri, A. R., Lestari, I., Permana, E., Ekasari, M., and Rasyid, N. A. (2026). Optimization Depolymerization of Tilapia Fish Scale Chitosan by Oxidative Degradation with H_2O_2 using Central Composite Design (CCD). *ALCHEMY Jurnal Penelitian Kimia*, 22(1), 95-105. doi: https://dx.doi.org/10.20961.alchemy.22.1.95765.95-105.

high molecular weight through depolymerization using enzymatic degradation (Nurhaeni *et al*., 2019; Aktuganov and Melent'ev, 2017), acid hydrolysis (Wolf *et al*., 2023; Aljbour *et al*., 2019), and oxidative degradation (Seo *et al*., 2007). Oxidative degradation occurs much faster than acid hydrolysis and, moreover, enzymatic degradation. Some of the ingredients that have been used in this method are O_3, $NaNO_2$, and H_2O_2. However, H_2O_2 is more widely used because it is easy to use, readily available, and environmentally friendly, leaving no harmful residues (Tabassum *et al*., 2023; Tanasela *et al*., 2016). The effectiveness of H_2O_2 in lowering the molecular weight of chitosan has been reported in a number of studies, which showed a final molecular weight of 65 kDa (Binh *et al*., 2021); 4.8 kDa (Sheng *et al*., 2022); and 2 kDa (Nguyen *et al*., 2023), thus confirming its role as an efficient degradation agent.

In the oxidative degradation method, the molecular weight of chitosan decreases sharply at the beginning of the reaction, but as the reaction time increases, the change in oligochitosan molecular weight becomes insignificant (Kadambayevich *et al*., 2021). Therefore, efficiency in this method is indispensable for determining the optimal conditions of its reaction factors, such as temperature, time, and H_2O_2 concentration. A statistical approach can be taken to determine such optimal conditions. One statistical approach that can be used is the Central Composite Design (CCD), which can predict responses across various conditions, reduce the number of experiments required, and enable the use of surface response graphs to visualize the influence of variables on the response (Kamboj *et al*., 2022). Several studies have reported that this method is excellent in determining optimal conditions in pharmaceuticals (Somadasan *et al*., 2024), biotechnology (Araujo and Silva, 2024), food (Nainggolan *et al*., 2023), and chemical analysis (Necer *et al*., 2024).

RESEARCH METHODS

The ingredients used in this study were tilapia scales, NaOH (Merck), HCl 37% (Merck), methanol (Merck), acetic acid (Merck), H_2O_2 30% (Merck), potassium ferrisianide ($K_3[Fe(CN)_6]$), Na_2CO_3, and standard D-glucosamine hydrochloride. Meanwhile, the tools used include a magnetic stirrer, sieve, hotplate, analytical balance, measuring cup, chemical beaker, blender, mortar and pestle, Fourier Transform Infrared (FTIR) Bruker ALPHA II, and X-Ray Diffraction (XRD) XPERT PRO PANalytical.

Sample Preparation

Tilapia scale samples were washed clean with water, then dried in the sunlight until dry. Before being mashed, tilapia scales are ovened for 30 minutes at 50 °C. The dried tilapia scales were mashed using the High Speed Multi Function Grinder and then sifted through a 100-mesh sieve to obtain a uniform sample size.

Chitin Extraction and Isolation Stages

Demineralization

A total of 12 g of samples was added to 240 mL of 0.5 M HCl solution. The demineralization results were filtered, washed with water until neutral, and dried in an oven at 40 °C (Alcalde and Fonseca, 2016).

Deproteinization

The demineralized sample was added to 100 mL of 0.5% NaOH solution (10:2) while stirring at 50 °C for 3 hours. After that, the sample was filtered, washed with water until neutral, and dried in an oven at 40 °C (Alcalde and Fonseca, 2016).

Deacetylation Stage

A total of 10 g of chitin was added to 400 mL of 40% NaOH solution. The solution was stirred for 6 hours at 117 °C. The solution was filtered to separate the solids, then the solids were washed with water until the pH was neutral. After that, the solids were washed with 30 mL of methanol and dried in an oven at 40 °C (Alcalde and Fonseca, 2016).

Chitosan Characterization Stage

The chitosan obtained was characterized by ninhydrin assays, and its moisture content, ash content, molecular weight, and degree of deacetylation were determined by FTIR.

Chitosan Depolymerization Stage

A total of 2.0 g of chitosan was placed in the Erlenmeyer flask, then 100 mL of 0.5% HCl was added. Next, 50 mL of H_2O_2 is added, left for 10 minutes, and heated. The treatment data from the variation in H_2O_2 concentration, heating temperature, and reaction time used are shown in Table 1. This treatment data is the result of a design from the Design-Expert 13 software with α value of 1.68179, covering 14 non-center points and 6 center points. After that, the solution was cooled to room temperature, and NaOH was added until it was neutral. The insoluble chitosan residues were separated by filtration. Next, the solution was evaporated with a rotary evaporator and dried. The resulting solids were oven-dried at 40 °C.

Table 1. Chitosan depolymerization treatment data.

Run	A= Concentration (M)	B= Temperature (°C)	C= Time (Hours)
1	1	70	1
2	3.6	50	2
3	2	50	2
4	2	83.6359	2
5	2	50	2
6	2	50	2
7	1	70	3
8	0.3	50	2
9	2	50	2
10	2	50	0.75
11	1	50	3
12	2	50	2
13	3	30	1
14	2	16.3641	2
15	3	30	3
16	2	50	2
17	3	70	1
18	1	30	1
19	3	70	3
20	2	50	3.42

Determination of Molecular Weight

The color reagent was prepared by dissolving 0.5 g of potassium ferrisianide in 1 L of 0.5 M sodium carbonate and storing it in a brown bottle. A standard solution of D-glucosamine hydrochloride (GAH) was prepared by dissolving 1 g of GAH in 100 mL of deionized water. Standard curves were created by mixing various volumes of GAH standard solution with 2 mL of color reagent in a closed tube, then adjusting the volume to exactly 5 mL with deionized water. After that, the tube was closed and heated in boiling water for 15 minutes, and cooled to room temperature. Furthermore, its absorbance was measured using a UV-Vis spectrophotometer at 420 nm. The same method was performed for oligochitosan samples (Tanasale *et al.*, 2019). The average molecular weight (M_n) of oligochitosan is calculated using Equation 1.

$$M_n = \frac{W_1}{W_2} \times 215{,}5 \quad (1)$$

Description:
W_1 = weight of oligochitesone (g)
W_2 = the amount of GAH equivalent to the oligochitosan absorbance of the standard curve (g)

Stages of Oligochitosan Characterization

The molecular weight of the depolymerized chitosan was statistically analyzed using the CCD method to determine its optimal condition. The optimum conditions obtained were used in the advanced depolymerization process, followed by characterization using FTIR and XRD, as well as solubility analysis.

RESULTS AND DISCUSSION

Isolation of Chitin Scales of Tilapia

The demineralization process in this study was carried out to remove mineral content from fish scales and obtain chitin with a higher level of purity. The demineralization method uses an HCl solution, chosen for its strong

acidity, which dissolves calcium salts such as $CaCO_3$ and $Ca_3(PO_4)_2$, the main minerals in fish scales. The reaction between the mineral and the Cl ions in HCl produces mineral salts (Ramadhani and Firdhausi, 2021). Nurmala *et al.* (2018) report that the demineralization process was characterized by the appearance of CO_2 gas bubbles, indicating the occurrence of a reaction between HCl and mineral salts in fish scales (Figure 1).

Figure 1. Demineralization process.

The chemical reactions that occur in the demineralization process are shown in Reactions 1 and 2.

$Ca_3(PO_4)_{2(s)} + 6HCl_{(aq)} \rightarrow 3CaCl_{2(aq)} + 2H_3PO_{4(aq)}$ (Reaction 1)

$CaCO_{3(s)} + 2HCl_{(aq)} \rightarrow CaCl_{2(aq)} + H_2O + CO_{2(g)}$ (Reaction 2)

Based on the chemical reactions, calcium carbonate is removed, yielding two products: calcium chloride, which is soluble in water and is lost during the washing process (Reaction 1), and carbon dioxide, which is released as a gas (Reaction 2).

After demineralization, deproteinization is performed to separate or release protein bonds in fish scales using a NaOH solution. In this process, the alkaline NaOH reacts with proteins in fish scales to produce a soluble sodium proteinate. This demineralization and deproteinization process yields 54.36% chitin from dried tilapia scales.

Deacetylation and Chitosan Scales of Tilapia

An important stage in the manufacture of chitosan is the deacetylation process, which removes the acetyl group ($–COCH_3$) from chitin using an alkaline solution, forming an amine group ($–NH_2$) (Setiati *et al.*, 2021). To confirm the success of this deacetylation process, a ninhydrin test was performed to qualitatively demonstrate that acetamide groups in chitin were deacetylated to form amine groups. The ninhydrin test is considered positive if it produces a purple solution (Figure 2).

Figure 2. Ninhydrin test.

Ninhydrin is a strong oxidizer that will react with the chitosan amine group at pH 4 – 8 to form a bonding compound between ninhydrin and hydrandin via a purple nitrogen bridge, as shown in Reaction 3 (Imtihani and Permatasari, 2020).

$R–NH_2 + C_9H_6O_4 \rightarrow$ Purple color product $+ H_2O_{(g)}$ (Reaction 3)

The results of the characterization of the chitosan functional group using FTIR in this study showed an absorption band at 3000 – 3600 cm^{-1}, corresponding to the stretching vibrations of O–H and N–H, with a peak at 3267 cm^{-1}. The stretching vibration C–H is observed in the wavenumber range of 2800 – 3000 cm^{-1}, with a peak at 2921 cm^{-1}. The bending vibration of the C–H bond is observed at 1412 cm^{-1}. The characteristic of chitosan compounds is shown by absorption in the 1500 – 1650 cm^{-1} region, with a peak at 1585 cm^{-1}, which corresponds to the bending vibration of the N–H group. The change in the functional group from chitin to chitosan is evidenced by the absorption band at 1627.72 cm^{-1}, which corresponds to the elongated vibration of C=O and shows a decrease in intensity after deacetylation. This is because the secondary N–H amide group present in the structure of the chitin molecule is reduced due to the release of the acetyl group and the formation of an amine group (NH_2) in chitosan (Hsu *et al.*, 2015). The FTIR results for chitin and chitosan are shown in Figure 3.

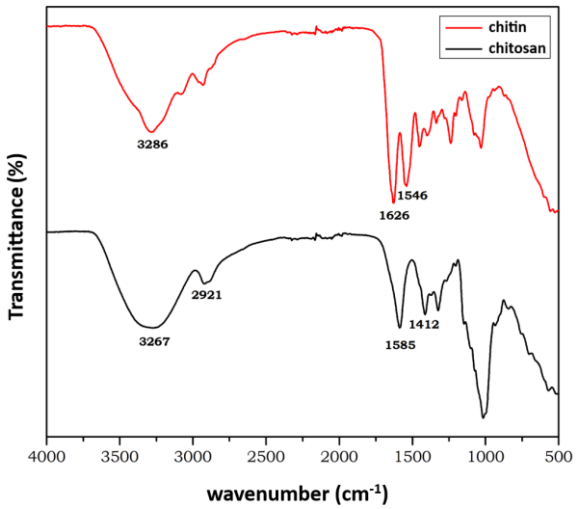

Figure 3. Results of FTIR chitin and chitosan.

Chitosan from tilapia scales is characterized by its degree of deacetylation and molecular weight. The degree of deacetylation of chitosan from tilapia scales was determined using the baseline method, while the molecular weight was determined by flow rate. The results of the calculation indicated that the degree of deacetylation and molecular weight of chitosan from tilapia scales were 74.24% and 264.214 kDa, respectively.

Optimization of the Depolymerization of Chitosan Scales of Tilapia

The oligochitosan (low-molecular-weight chitosan) obtained in this study was analyzed for molecular weight using the End Group Analysis method. The determination is made by first preparing a standard curve using a standard solution of D-glucosamine hydrochloride with potassium ferricyanide as the dye reagent. The selection of D-glucosamine hydrochloride as the standard was based on the similarity of the hydroxyl hemiacetal group to the oligochitosan, allowing both to react with potassium ferrisianide, resulting in a measurable colored complex (Tanasale *et al.*, 2016). The standard curve shows an excellent linear relationship with a regression equation of y = 0.5345x – 0.0204 and a determination coefficient (R^2) of 0.9963, as shown in Figure 4.

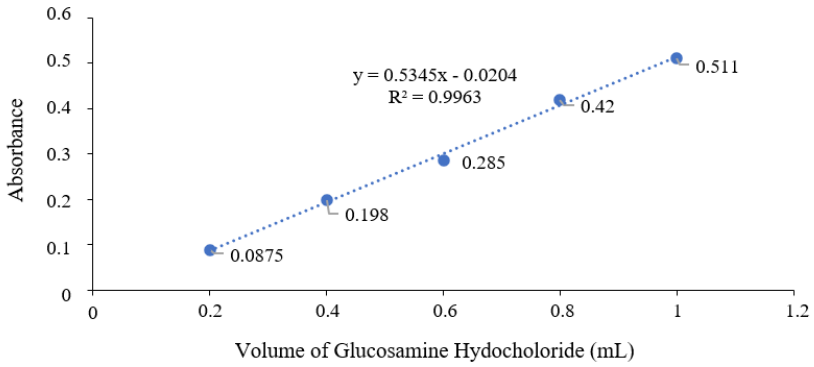

Figure 4. Standard curve of glucosamine hydrochloride.

Optimization is carried out to facilitate the preparation and interpretation of the data obtained, while minimizing the cost of using raw materials and maximizing the desired results. One effective method for independent variable optimization is the Central Composite Design (CCD). This method is used to determine the ideal setting for optimal results. CCD can overcome the limitations of trial-and-error methods and is the preferred method for optimizing target values (Suryani *et al.*, 2022).

The results of the CCD calculation indicate that the best-performing models are linear. The model's accuracy is evident from the lack-of-fit test. The lack-of-fit value is 0.0147, indicating that the model is appropriate and accurate. This is also shown by the lack-of-fit value of <0.05, which indicates a good model according to statistical criteria. The R^2 value from the CCD analysis itself was 0.8748. These results are good because the R^2 value is close to 1, indicating that the response (oligochitosan molecular weight) is strongly influenced by the independent variables of concentration, temperature, and time.

Table 2. Analysis of variance (ANOVA) for linear models of CCD results.

Source	Sum of Squares	df	Mean Square	F-value	p-value	
Models	3.446 × 107	3	1.149 × 107	37.25	< 0.0001	Significant
A-Concentration	2.841 × 107	1	2.841 × 107	92.12	< 0.0001	
B-Temperature	3.244 × 106	1	3.244 × 106	10.52	0.0051	
C-Time	2.810 × 106	1	2.810 × 106	9.11	0.0082	

The accuracy of each parameter, based on its significance to the response, is shown in Table 2. The results showed the overall accepted significance level is $p < 0.0001$. The details of the inaccuracies are as follows: the concentration parameter has a p-value < 0.0001, while the temperature and time parameters have p-values of 0.0051 and 0.0082, respectively. According to Hendrawan *et al*. (2016), the response is considered significant if the P value is less than 5%. In addition, the F value in the model is 37.25, indicating that the model is significant. Therefore, there is only a 0.01% chance that an F value of this magnitude could occur due to noise; thus, it can be said that the model was not obtained by chance.

The results of the CCD model calculation, evaluated across all factors, indicated that the model produced the optimal prediction at an H_2O_2 concentration of 3.6 M, a temperature of 50 °C, and a reaction time of 2 hours. The result will result in a molecular weight of 3.093 kDa. These results show that the H_2O_2 -mediated depolymerization process successfully produces oligochitosan with a low molecular weight. Compared with previous studies, the final molecular weight obtained was comparable or higher, namely 4.8 kDa (Sheng *et al*., 2022) and 2 kDa (Nguyen *et al*., 2023). These results show that the optimization conditions obtained using the CCD method produce oligochitosan products with characteristics comparable to those reported in previous studies.

The linear model equation obtained from the optimization analysis of chitosan depolymerization conditions on the molecular weight response is shown in Equation 2.

$$Mn = 8120{,}75 - 1442{,}28\ A - 24{,}37\ B + 435{,}591\ C \quad (2)$$

Based on the results of this CCD calculation, a 3D graph of the influence of concentration, temperature, and time on the response shown in Figure 5 was also obtained.

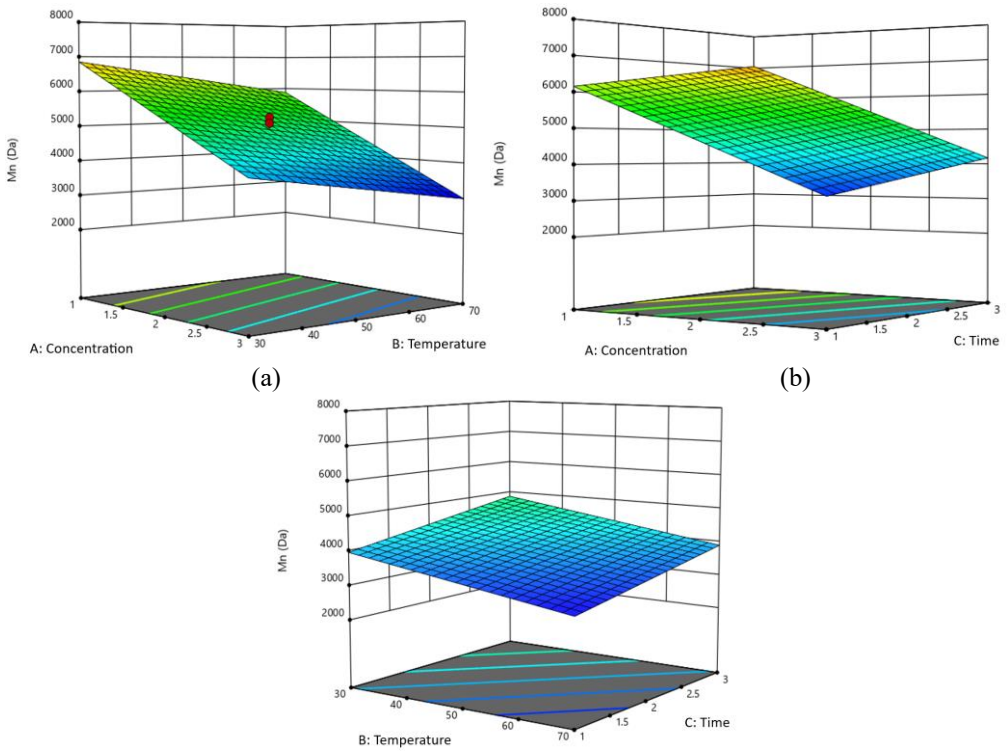

Figure 5. The 3D graph results of the CCD calculation (a) concentration with temperature, (b) concentration with time, and (c) temperature with time.

Based on the CCD calculation, a perturbation plot was generated (Figure 6), showing the change in response when one factor varies around the reference point while the other is held at the reference value. The line's slope indicates how strongly the factor influences changes in the response. affects the change in response. A steep line indicates a more influential factor, and a slope sign indicates the direction of influence. Line A has the steepest slope and decreases from left to right, indicating an increase in H_2O_2 concentration and a noticeable decrease in the chitosan molecule's weight. This shows that H_2O_2 concentration is the most important factor in reducing molecular weight during depolymerization. The B line is also decreasing, but more sloping in the same direction as the A line, indicating that the depolymerization temperature exerts a moderate effect on the decrease in the weight of the chitosan molecule. Meanwhile, the C line is slightly up, indicating that the depolymerization time exerts a small influence.

H_2O_2 produces oxygen radicals (·OH) during the depolymerization reaction, which will promote more effective termination of the chitosan chain than increases in temperature and time within the test range. Therefore, the concentration of H_2O_2 can accelerate the chitosan chain-cleavage reaction, leading to a marked decrease in chitosan molecular weight (Zheng *et al*., 2022). Meanwhile, temperature and time affect kinetics, but their effects are relatively small because the availability of H_2O_2 controls the selected reaction range or trajectory (Purwanto *et al*., 2019).

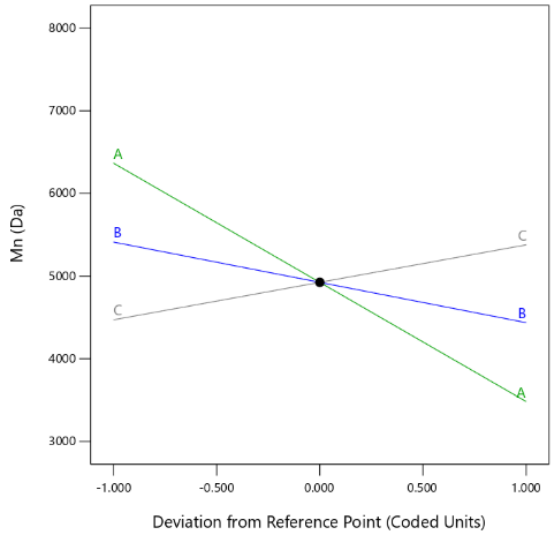

Figure 6. Perturbation graph.

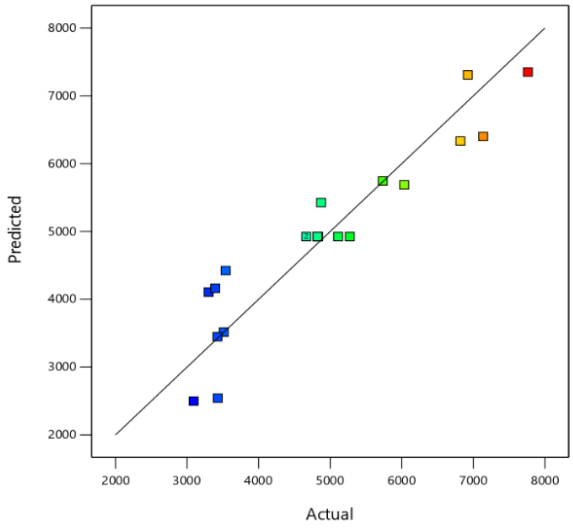

Figure 7. A comparison graph of predicted and actual values of the CCD.

Based on the CCD calculation, a graph was generated showing the molecular weight predictions from the CCD and the actual molecular weight of the depolymerization obtained in the study. The results of the graph are shown in Figure 7. Figure 7 shows the relationship between the molecular weight predicted by the CCD model and the experimental results for chitosan depolymerization of tilapia scales. The data points scattered around the diagonal line indicate that the prediction model shows a good degree of agreement with the experimental data. The closer the point is to the diagonal line, the smaller the deviation between the actual value and the prediction. The relatively even distribution of points around the line also indicates that the model can predict with high accuracy across a wide range of data. This is reinforced by a high coefficient of determination (R^2) of 0.8513, indicating a valid and reliable model for determining the optimal process conditions (Bezerra *et al*., 2008).

Oligochitosan Characterization

The product resulting from the chitosan depolymerization process in this study was characterized by FTIR to confirm that the depolymerized product is oligochitosan, which has the same FTIR absorption profile as chitosan (Figure 8). This similarity in absorption suggests that oligochitosans lack structural damage, despite their differing molecular weights.

Identification of crystalline and amorphous particles to determine the crystallinity index of chitosan and oligochitosan was performed using XRD (Figure 9). The crystallinity index for chitosan was 84.34%, while that for oligochitosan was 59.17%. Suryani *et al.* (2022) state that oligochitosan with a lower crystallinity index or

oligochitosan with increasingly amorphous structures will have greater solubility in water. This is because amorphous structures have looser molecular chains than crystalline structures, creating more intermolecular space that allows water molecules to enter, interact with oligochitosan chains, and dissolve them.

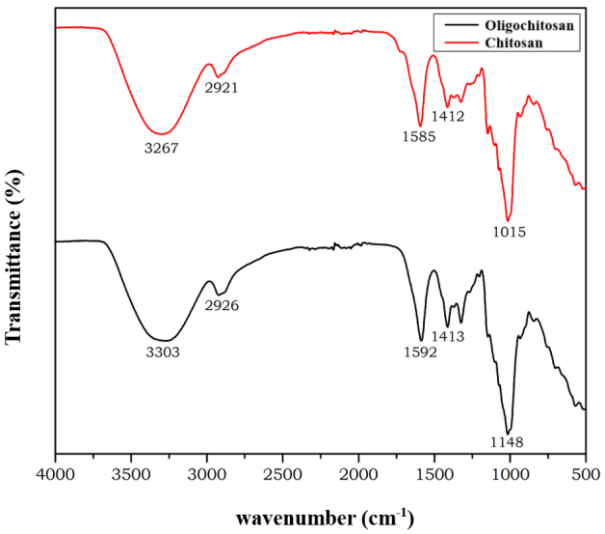

Figure 8. Comparison chart of FTIR spectra of oligochitosan and chitosan from fish scales.

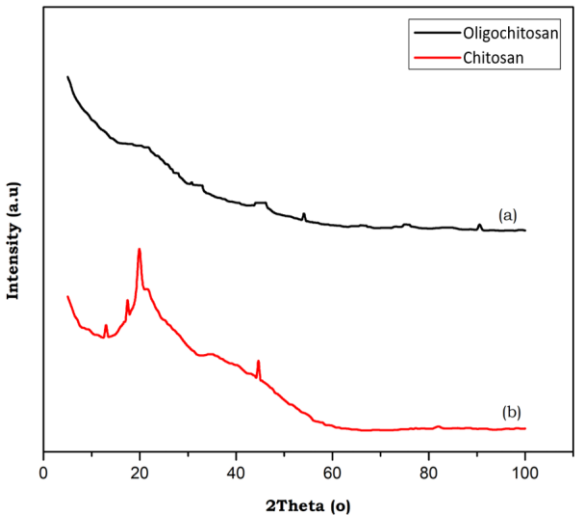

Figure 9. The diffraction pattern of XRD is (a) oligochitosan and (b) chitosan tilapia scales.

Identification of crystalline and amorphous particles to determine the crystallinity index of chitosan and oligochitosan was performed using XRD (Figure 9). The crystallinity index for chitosan was 84.34%, while that for oligochitosan was 59.17%. Suryani *et al.* (2022) state that oligochitosan with a lower crystallinity index or oligochitosan with increasingly amorphous structures will have greater solubility in water. This is because amorphous structures have looser molecular chains than crystalline structures, creating more intermolecular space that allows water molecules to enter, interact with oligochitosan chains, and dissolve them.

The oligochitosan products produced in this study are also characterized by solubility at neutral pH. This solubility is an important parameter for distinguishing chitosan and oligochitosan. This happens because chitosan is insoluble in water at neutral pH, whereas oligochitosan is highly soluble at neutral pH (Pari *et al.,* 2022). Oligochitosan solubility was characterized in this study by dissolving oligochitosan in water at neutral pH for 30 minutes. A comparison of the solubility results from this study is shown in Figure 10. The solubility of oligochitosan in water with a neutral pH in this study was 100%. The results are also the same as those of Pari *et al.* (2022), who found that chitosan depolymerized by three different methods dissolves completely in water at neutral pH.

Figure 10. The difference in the solubility test results of (a) oligochitosan and (b) chitosan from tilapia scales.

CONCLUSION

The chitosan yield obtained from the tilapia chitin deacetylation process was 54.36%, with a degree of deacetylation of 74.24% and a molecular weight of 264.214 kDa. The optimal conditions predicted using Central Composite Design (CCD) for the chitosan depolymerization process in this study are 3.6 M concentration, 50 °C temperature, and 2 hours, with a molecular weight of 4.093 kDa. The analysis of the depolymerization results from this study shows that the most influential factor in oligochitosan production is H_2O_2 concentration. The

characterization of oligochitosan includes measurements of crystallinity and solubility, indicating that it exists in an amorphous form and dissolves completely in water.

CONFLICT OF INTEREST

There are no conflicts of interest in this article.

AUTHOR CONTRIBUTION

DEW dan ARP: Conceptualization, Methodology, Data Analysis, Manuscript Draft Writing; IL, EP, and ME: Manuscript Review and Editing; NAR: Data Methodology and Analysis.

ACKNOWLEDGEMENT

The author would like to thank the parties who assisted in completing this research, especially the University of Jambi, which funded it through the PNBP scheme of the Faculty of Science and Technology under the Penelitian Dosen Pemula scheme.

DAFTAR PUSTAKA

Aktuganov, G.E., and Melent'ev, A.I., 2017. Specific Features of Chitosan Depolymerization by Chitinases, Chitosanases, and Nonspecific Enzymes in the Production of Bioactive Chitooligosaccharides (Review). *Applied Biochemistry and Microbiology*, 53. https://doi.org/10.1134/S0003683817060023.

Alcalde, L.B., and Fonseca, G.G., 2016. Alkali Process for Chitin Extraction and Chitosan Production from Nile Tilapia (*Oreochromis niloticus*) Scales. *Latin American Journal of Aquatic Research*, 44, 683–688. https://doi.org/10.3856/vol44-issue4-fulltext-3.

Aljbour, N.D., Beg, M.D.H., and Gimbun, J., 2019. Acid Hydrolysis of Chitosan to Oligomers Using Hydrochloric Acid. *Chemical Engineering and Technology*, 42, 1741–1746. https://doi.org/10.1002/ceat.201800527.

Araujo, T.F., and Silva, L.P., 2024. The Utilization of Central Composite Design for the Production of Hydrogel Blends for 3D Printing. *Coatings*, 14. https://doi.org/10.3390/coatings14101324.

Bezerra, M.A., Santelli, R.E., Oliveira, E.P., Villar, L.S., and Escaleira, L.A., 2008. Response Surface Methodology (RSM) as a Tool for Optimization in Analytical Chemistry. *Talanta*, 76, 965–977. https://doi.org/10.1016/j.talanta.2008.05.019.

Binh, N.T.T., Bao, H.N.D., Prinyawiwatkul, W., and Trung, T.S., 2021. Antioxidative and Antimicrobial Effects of Low Molecular Weight Shrimp Chitosan and Its Derivatives on Seasoned-Dried Pangasius Fillets. *International Journal of Food Science and Technology*, 56, 5119–5229. https://doi.org/10.1111/ijfs.15280.

Hendrawan, Y., Susilo, B., Putranto, A.W., Riza, D.F.A., Maharani, D.M., and Amri, M.N., 2016. RSM-CCD Algorithm for Optimizing Waterjet Vacuum Evaporator Using Fuzzy Temperature Control in The Milk Candy Production. *AGRITECH*, 36, 226-232. https://doi.org/10.22146/agritech.12868.

Hsu, C.H., Chen, S.K., Chen, W.Y., Tsai, M.L., and Chen, R.H., 2015. Effect of the Characters of Chitosans Used and Regeneration Conditions on the Yield and Physicochemical Characteristics of Regenerated Products. *International Journal of Molecular Sciences*, 16, 8621–8634. https://doi.org/10.3390/ijms16048621.

Imtihani, H.N., and Permatasari, S.N., 2020. Sintesis dan Karakterisasi Kitosan dari Limbah Kulit Udang Kaki Putih (*Litopenaeus vannamei*). *SIMBIOSA*, 9, 129-137. https://doi.org/10.33373/sim-bio.v9i2.2699.

Kadambayevich, P.K., Evgenievich, T. V, and Sharafovna, R.S., 2021. Oligochitosan and Oligochitosan Ascorbat: Preparation and Properties. *International Journal of Modern Agriculture*, 10, 1244–1262.

Kamboj, A., Chopra, R., Singh, R., Saxena, V., and GV, P.K., 2022. Effect of Pulsed Electric Field Parameters on the Alkaline Extraction of Valuable Compounds from Perilla Seed Meal and Optimization by Central Composite Design Approach. *Applied Food Research*, 2. https://doi.org/10.1016/j.afres.2022.100240.

Mahardika, R.G., Jumnahdi, M., and Widyaningrum, Y., 2020. Deasetilasi Kitin Cangkang Rajungan (*Portunus pelagicus*) menjadi Kitosan Menggunakan Iradiasi Microwave. *Al-Kimia*, 8, 149–158. https://doi.org/10.24252/al-kimia.v8i2.7999.

Nainggolan, E.A., Banout, J., and Urbanova, K., 2023. Application of Central Composite Design and Superimposition Approach for Optimization of Drying Parameters of Pretreated Cassava Flour. *Foods*, 12. https://doi.org/10.3390/foods12112101.

Necer, I.L., Oukebdane, K., and Didi, M.A., 2024. Central Composite Design Optimization Study of the Sorption of Bemacid Blue Anthraquinone Dye by Fe_3O_4-Bentonite from a Cupric Medium. *International Journal of Environmental Analytical Chemistry*, 104, 1994–2013. https://doi.org/10.1080/03067319.2022.2054709.

Nguyen, T.H.P., Le, N.A.T., Tran, P.T., Bui, D. Du, and Nguyen, Q.H., 2023. Preparation of Water-Soluble Chitosan Oligosaccharides by Oxidative Hydrolysis of Chitosan Powder with Hydrogen Peroxide. *Heliyon*, 9, e19565. https://doi.org/10.1016/j.heliyon.2023.e19565.

Nurhaeni, N., Ridhay, A., and Laenggeng, A.H., 2019. Depolymerization of Chitosan from Snail (*Pilla ampullaceae*) Field Shell Using α-Amylase, in: *Journal of Physics: Conference Series*. https://doi.org/10.1088/1742-6596/1242/1/012005.

Nurmala, N.A., Susatyo, E.B., and Mahatmanti, F.W., 2018. Sintesis Kitosan dari Cangkang Rajungan Terkomposit Lilin Lebah dan Aplikasinya sebagai *Edible Coating* pada Buah Stroberi. *Indonesian Journal of Chemical Science*, 7.

Pari, R.F., Mayangsari, M., and Hardiningtyas, S.D., 2022. Spektrum Gugus Fungsi FTIR Oligokitosan pada Setiap Perlakuan Memiliki Gugus Fungsi yang Sama seperti pada Kitosan. *Jurnal Pengolahan Hasil Perikanan Indonesia (JPHPI)*, 24, 118–131.

Purwanto, E., Connor, J., and Ngothai, Y., 2019. The Kinetics Oxidative Degradation of Chitosan in Formic Acid with the Presence of Hydrogen Peroxide, in: *IOP Conference Series: Materials Science and Engineering*. https://doi.org/10.1088/1757-899X/703/1/012041.

Ramadhani, A.A., and Firdhausi, N.F., 2021. Potensi Limbah Sisik Ikan Sebagai Kitosan dalam Pembuatan Bioplastik. *Jurnal Al-Azhar Indonesia Seri Sains dan Teknologi*, 6. https://doi.org/10.36722/sst.v6i2.782.

Saleh, J., Budi, S., and Salam, S., 2021. *Pengembangan Budidaya Ikan Nila*. Pusaka Almaida, Sulawesi Selatan.

Seo, S., King, J.M., and Prinyawiwatkul, W., 2007. Simultaneous Depolymerization and Decolorization of Chitosan by Ozone Treatment. *Journal of Food Science*, 72. https://doi.org/10.1111/j.1750-3841.2007.00563.x.

Setiati, R., Siregar, S., Wahyuningrum, D., and Rinanti, A., 2021. Synthesis Method of Chitin Become Chitosan Polymer from Shrimp Shells for Enhanced Oil Recovery. *IOP Conference Series: Earth and Environmental Science*, 737, 012048. https://doi.org/10.1088/1755-1315/737/1/012048.

Sheng, Z., Guo, A., Wang, J., and Chen, X., 2022. Preparation, Physicochemical Properties and Antimicrobial Activity of Chitosan from Fly Pupae. *Heliyon*, 8, e11168. https://doi.org/10.1016/j.heliyon.2022.e11168.

Somadasan, S., Subramaniyan, G., Athisayaraj, M.S., and Sukumaran, S.K., 2024. Central Composite Design: An Optimization Tool for Developing Pharmaceutical Formulations. *Journal of Young Pharmacists*, 16, 400–409. https://doi.org/10.5530/jyp.2024.16.52.

Suryani, S., Chaerunisaa, A.Y., Joni, I.M., Ruslin, R., Ramadhan, L.O.A.N., Wardhana, Y.W., and Sabarwati, S.H., 2022. Production of Low Molecular Weight Chitosan Using a Combination of Weak Acid and Ultrasonication Methods. *Polymers*, 14, 1–15. https://doi.org/10.3390/polym14163417.

Susanti, N., and Purwanti, A., 2020. Pembuatan Kitosan dari Limbah Sisik Ikan (Variabel Konsentrasi Larutan NaOH dan Waktu Ekstraksi). *Jurnal Inovasi Proses*, 5, 40–45.

Tabassum, N., Ahmed, S., Ittisaf, M.M., Rakid-Ul-Haque, M., and Ali, M.A., 2023. A Green Approach for Depolymerization of Chitosan: Applications in Hydrogels. *Cellulose*, 30, 8769–8787. https://doi.org/10.1007/s10570-023-05372-9.

Tanasale, M.F.J.D.P., Telussa, I., Sekewael, S.J., and Kakerissa, L., 2016. Extraction and Characterization of Chitosan from Windu Shrimp Shell (*Penaeus monodon*) and Depolymerization Chitosan Process with Hydrogen Peroxide Based on Heating Temperature Variations. *Indonesian Journal of Chemical Research*, 3, 308–316.

Wolf, M., Hanstein, S., Schmitz, O., Czermak, P., and Ebrahimi, M., 2023. Depolymerization of Hemicelluloses Utilizing Hydrothermal and Acid Catalyzed Processes Proceed by Ultrafiltration as Fractionation Media. *Carbohydrate Polymer Technologies and Applications*, 6. https://doi.org/10.1016/j.carpta.2023.100355.

Zheng, H., Cui, S., Sun, B., Zhang, B., Tao, D., Wang, Z., Zhang, Y., and Ma, F., 2022. Synergistic Effect of Discrete Ultrasonic and H_2O_2 on Physicochemical Properties of Chitosan. *Carbohydrate Polymers*, 291, 119598. https://doi.org/10.1016/j.carbpol.2022.119598.